THE JOURNAL OF PHYSICAL CHEMISTRY B

Article

pubs.acs.org/JPCB

Quantitative Prediction of Physical Properties of Imidazolium Based Room Temperature Ionic Liquids through Determination of Condensed Phase Site Charges: A Refined Force Field

Anirban Mondal and Sundaram Balasubramanian*

Chemistry and Physics of Materials Unit, Jawaharlal Nehru Centre for Advanced Scientific Research, Bangalore 560 064, India

Supporting Information

ABSTRACT: Quantitative prediction of physical properties of room temperature ionic liquids through nonpolarizable force field based molecular dynamics simulations is a challenging task. The challenge lies in the fact that mean ion charges in the condensed phase can be less than unity due to polarization and charge transfer effects whose magnitude cannot be fully captured through quantum chemical calculations conducted in the gas phase. The present work employed the density-derived electrostatic and chemical (DDEC/c3) charge partitioning method to calculate site charges of ions using electronic charge densities obtained from periodic density functional theory (DFT) calculations of their crystalline phases. The total ion charges obtained thus range between −0.6e for chloride and −0.8e for the PF_6 ion. The mean value of the ion charges obtained from DFT calculations of an ionic liquid closely matches that obtained from the corresponding crystal thus confirming the suitability of using crystal site charges in simulations of liquids. These partial charges were deployed within the well-established force field developed by Lopes et al., and consequently, parameters of its nonbonded and torsional interactions were refined to ensure that they reproduced quantum potential energy scans for ion pairs in the gas phase. The refined force field was employed in simulations of seven ionic liquids with six different anions. Nearly quantitative agreement with experimental measurements was obtained for the density, surface tension, enthalpy of vaporization, and ion diffusion coefficients.

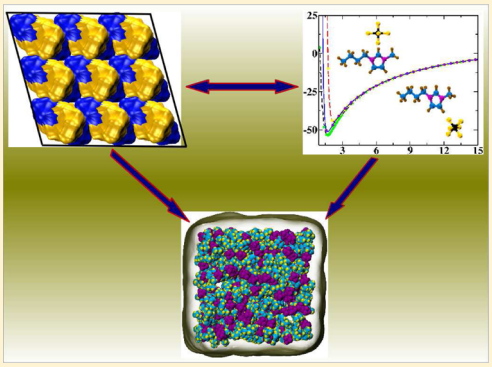

INTRODUCTION

In recent years, room temperature ionic liquids (ILs) have engaged the attention of many researchers as they are fluids with wide ranging applications. Due to their unique properties such as low melting points, negligible to low vapor pressure, nonflammability, and good ionic conductivity, the possibility of manifold applications in catalysis, electrochemistry, separation technologies, and nanoparticle syntheses or as performance chemicals has stimulated extensive study on this class of compounds during the past decade.[1−16]

Molecular simulation methods have been widely used to obtain atomic-level understanding of room temperature ionic liquids. These include ab initio molecular dynamics (AIMD)[17−25] and molecular dynamics (MD) simulations using polarizable force fields[8,26−29] and those employing empirical potentials.[3,4,30−33] Although AIMD simulations can possibly provide an accurate picture of cation−anion hydrogen bonding and anion polarization, they are computationally expensive. Force fields that include terms that include ion polarizations do offer an improvement over those with fixed charges; however, they too can be computationally demanding and are not available for a wide class of compounds.

Nonpolarizable force fields for several ILs based on the imidazolium, pyridinium, and phosphonium cations were developed by Lopes, Padua, and co-workers using the OPLS-AA and AMBER framework.[34−38] In a similar approach, Wang and co-workers developed a force field for a few ILs based on the imidazolium cation.[39] Other force fields developed for ILs are a few united atom models,[40−42] the OPLS-AA model,[43] coarse grained models,[44−46] etc. Though many of them reproduce well the density and to a large extent the intermolecular structure, their ability to quantitatively reproduce surface tension and transport quantities such as the diffusion coefficient has been a matter of discussion.[47−53] Ludwig et al.[50] developed a force field for $[C_nMIM][NTf_2]$ that describes the thermodynamic and transport properties reasonably well, in particular for ILs with short alkyl tails.[54]

Properties of ILs such as their low vapor pressure, ionic conductivity, shear viscosity, etc. are largely determined by the electrostatic interactions between the ions. Charge transfer and polarization of ionic species determine their effective charges in bulk ILs. Thus, one observes a net decrease in the effective charges on ions in bulk liquids,[8,55,56] in good agreement with recent photoelectron spectroscopy experiments of Licence and co-workers.[57,58] Atomic charges used in many force fields have mostly been derived from quantum chemical calculations of an ion or an ion pair studied in gas phase. The charges calculated thus do not capture these condensed phase effects and their use

Received: January 10, 2014
Revised: March 6, 2014
Published: March 7, 2014

   dx.doi.org/10.1021/jp500296x | J. Phys. Chem. B 2014, 118, 3409−3422

often leads to overbinding of ions in bulk. Such an approach was also found to diminish values of diffusion coefficients of ions in the liquid phase, relative to experimentally determined values.[26,39,59−63]

Voth and co-workers introduced polarizable force fields for ILs to capture the effect of electronic polarizability in condensed phases of ILs,[26] which resulted in a much faster diffusion of ions compared with results using the nonpolarizable model. Borodin and co-workers have contributed significantly to the development of both polarizable and nonpolarizable force fields for several ILs whose prediction of properties are in quantitative agreement with experiments.[28,63−66] A simpler (mean field level) treatment of charge transfer and polarizability within a nonpolarizable force field model is to scale the overall atomic charges and allowing for ion charges to deviate from values of ±1 e. The dynamics in the liquid consequently speeds up due to the lower electrostatic binding and this procedure has been implemented for ionic liquids by several groups.[49,55,56] However, the scale factors used so far have been empirical in nature.

Koßmann et al.[67] have employed second-order Møller−Plesset perturbation theory (MP2) and density functional theory (DFT) techniques to study clusters of [MMIM][Cl] and obtained a reduced charge for the chloride ion of −0.823 e. An ab initio molecular dynamics simulation of liquid [MMIM]-[Cl] followed by a Mulliken population analysis of snapshots performed by Bühl et al.,[18] also yielded a reduced charge for the chloride anion to be between −0.7 and −0.8 e. More recently, Delle Site and co-workers developed a protocol to calculate atomic partial charges to account for bulk phase charge transfer and polarization.[68−70] They have carried out a liquid phase AIMD simulation and used the Blöchl[71] method to calculate site charges for snapshots selected from the CPMD trajectory.

Starting from CLaP parameters as an initial guess along with the atomic charges calculated using the Blöchl method, Holm et al. refined the force field for [MMIM][Cl].[72] The density of the simulated liquid reproduced the experimental value reasonably well. At low temperature, the calculated ionic conductivity overestimated the experimental value, but the deviation from experiment vanishes in the high temperature region. Very recently, Holm et al. described a design of transferable force field for $[MMIM]^+$, $[EMIM]^+$, and $[BMIM]^+$ cations with a combination of thiocyanate $[SCN]^-$, chloride $[Cl]^-$, and dicyanamide $[DCA]^-$ as anions.[73] A similar refinement procedure as before was adopted. However, the density of simulated liquid [EMIM][DCA] was less than the experimental value by about 5%, which was attributed to an artifact of reduced net charge. The ionic conductivity too was underestimated by 50%.

Although attractive, this approach requires a AIMD simulation of the liquid to be performed, which is forbidding due to the computational cost. In a recent work, Zhang and Maginn proposed a novel idea to calculate atomic site charges for an IL from its crystalline phase.[74] They fitted a periodic electrostatic potential for crystalline 1-*n*-butyl-3-methylimidazolium hexafluorophosphate ([BMIM][PF_6]) and 1-ethyl-3-methylimidazolium hexafluorophosphate ([EMIM][PF_6]) and derived atom charges from it. Using these charges within the General AMBER force field (GAFF) framework, they concluded that charges calculated from crystalline phases are better in reproducing the dynamics of ILs than those obtained using the Blöchl method or that from scaling the unit charges calculated from gas phase quantum chemical calculation of one ion pair.

The local coordination shell of a cation in an ionic liquid shares much commonality with its crystalline counterpart. One should thus be able to exploit this aspect and generalize the approach delineated by Zhang and Maginn[74] for other ionic liquids. In the present work, we present a direct and systematic method to derive atomic charges for imidazolium based room temperature ionic liquids. Motivated by the work of Zhang and Maginn, we come up with a consistent set of site charges for cations and anions in six different ionic liquids by studying their crystalline counterparts using density functional theory. We have employed the density-derived electrostatic and chemical (DDEC) charge partitioning method[75,76] to calculate atomic charges of ions. The DDEC/c3 method has been proven earlier to be very accurate to calculate charges for periodic systems. It has been used to calculate charges for various porous and nonporous periodic systems such as metal organic framework, zeolites, etc.[77,78] In the present work, dihedral and nonbonded interaction parameters have been refined by taking into consideration the revised charges. This procedure is shown to reproduce experimental density, heat of vaporization, surface tension, and ion diffusion coefficients for several ionic liquids in nearly a quantitative fashion.

The content of this work is divided into three parts. First, we present the procedure to calculate atomic site charges for different ILs. Second, the protocol to refine intra- and intermolecular parameters accommodating these new set of charges is described. In the last section, results of various properties obtained using this refined force field are compared against experimentally determined quantities.

METHODOLOGY AND SIMULATION DETAILS

The force field developed by Lopes, Padua, and co-workers (CLaP)[34−38] covers a wide range of ILs and it reproduces static properties reliably[48] and is thus widely used. However, transport properties such as diffusion coefficient (and thus electrical conductivity) appears to be underpredicted by this model.[48−51] Thus, we have chosen the CLaP force field as an initial framework for our refinement procedure. The bond and angle parameters of CLaP have been retained; however, the partial charges on the atoms have been derived using the DDEC/c3 method as applied to electron density of either crystals (whose experimentally determined structures are known) or liquids. The electron density itself was obtained using density functional theory (DFT) calculations. The proposed set of partial charges would have an effect on the short-range (SR) interactions and thus the nonbonded potential parameters too need to be refitted. Revision of the charges and nonbonded parameters demands a revision of dihedral parameters as the two are related through 1−4 interactions.

Derivation of Atomic Charges. 1-Alkyl-3-methylimidazolium based ionic liquids containing six different anions were considered for calculation of site charges. These were hexafluorophosphate (PF_6), tetrafluoroborate (BF_4), bis(trifluoromethylsulfonyl)imide (NTf_2), chloride (Cl), nitrate (NO_3), and trifluoromethanesulfonate or triflate (CF_3SO_3). For each anion, three ILs with different lengths of pendant alkyl tails ranging from methyl to butyl were chosen for the calculations.

The nomenclature used to describe sites on the imidazolium ring is shown in Figure 1.

dx.doi.org/10.1021/jp500296x | J. Phys. Chem. B 2014, 118, 3409−3422

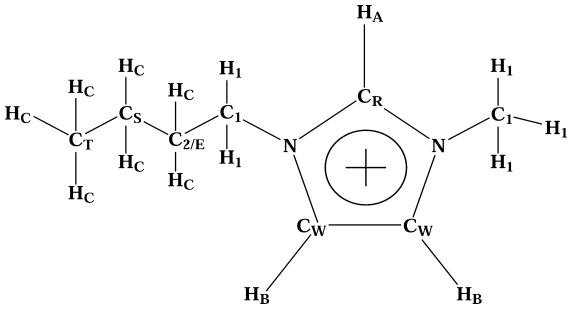

Figure 1. Atom labeling in the imidazolium ring.

Crystalline Phase Charges. Atomic charges were calculated from crystalline phases of ILs wherever experimental crystal structures are available. Initial cell parameters and atomic positions were taken from Cambridge crystal structure database.[79−81] The size of the simulation cell considered for all the crystals was 1 × 1 × 1. A description of all the systems studied here is provided in Table S1 of the Supporting Information.

Density functional theory (DFT) calculations were carried out using CP2K software.[82] All valence electrons were treated with triple-ζ double-polarized basis and a density cutoff of 280 Ry was used. Exchange and correlation effects were considered through the Perdew, Burke, and Ernzerhof (PBE) functional. Geodecker−Teter−Hutter (GTH) pseudopotentials[83] were used to consider the effect of core electrons and nuclei. Neither the coordinates nor the cell parameters were optimized. The wave functions were optimized with a convergence criterion of 10^{-7} on its gradient. Cube files of valence electron density were saved. DDEC charges were computed with the codes available at http://ddec.sourceforge.net as described by Manz and Sholl using the DDEC/c3 method.[75,76] We have tried to calculate atomic charges using some other methods also, such as Blöchl,[71] REPEAT,[84] and RESP.[85] However, charges obtained through these methods were not always consistent across different IL compounds and thus were discarded. A short discussion about these methods and results obtained from them is provided in the Supporting Information.

Charges Derived from the Liquid Phase. To check the transferability of the charges derived from a crystal and its corresponding liquid, simulations of the liquid phase were also carried out with the following protocol. A number of snapshots were chosen from a classical molecular dynamics (MD) simulation of an IL, carried out primarily using the CLaP force field. Liquid [BMIM][BF_4] alone was modeled using the Wang force field.[39] These configurations were then taken into DFT framework. The basis set, density cutoff, and pseudopotentials used were the same as mentioned previously. For each of these configurations, the gradient of the electronic wave functions and the force on the nuclei were optimized with convergence criteria of 10^{-7} and 10^{-3}, respectively. With these quenched configurations, atomic charges were calculated following the same procedure as described earlier for crystal systems. The charges thus obtained were averaged over all ions and configurations. Typical system sizes in these liquid simulations were around 30−40 ion pairs. A full description of these systems is provided in Table S2 in the Supporting Information.

The force field developed by Lopes and co-workers[34−37] was employed and MD simulations were carried out using the LAMMPS[86] software package. Furthermore, because the interaction cutoff has to be less than half box length, we have used a pairwise cutoff distance of 10 Å in these classical MD simulations. Initial positions of all atoms were generated by placing the molecules randomly in a box of length 20 Å. Equations of motion were integrated with the velocity Verlet algorithm with a time step of 1 fs. All C−H covalent bonds were constrained using the SHAKE algorithm as implemented in LAMMPS software.[86] Long range electrostatic interactions were computed using the particle−particle particle-mesh (PPPM) solver with a precision of 10^{-5}. As prescribed in the force field, a multiplication factor of 0.5 was used to scale down the nonbonded interactions calculated for a pair of atoms separated by three bonds. The parameters for cross interactions between different molecular species (atomic groups) were derived using standard Lorentz−Berthelot rules.[87] Cubic periodic boundary conditions were applied.

Constant-pressure and constant-temperature ensemble (*NPT*) simulations were carried out until the volume converged. The temperature and pressure of the system were maintained at 300 K and 1 atm using a Nóse−Hoover thermostat and barostat, respectively, with a damping factor of 1 ps. The densities of the systems compared well against experimental data. The final coordinates of the *NPT* run were taken to the constant-volume and constant-temperature (*NVT*) ensemble for a further equilibration for 5 ns under constant *NVT* conditions. Finally, an analysis run was generated for 10 ns. Configurations at every 1 ns were selected for coarse geometry optimization within DFT (as described earlier) and further for the calculation of atomic charges using the DDEC/c3 method.

Optimization of Short-Range Interactions. The accurate representation of short-range (SR) interactions is quite

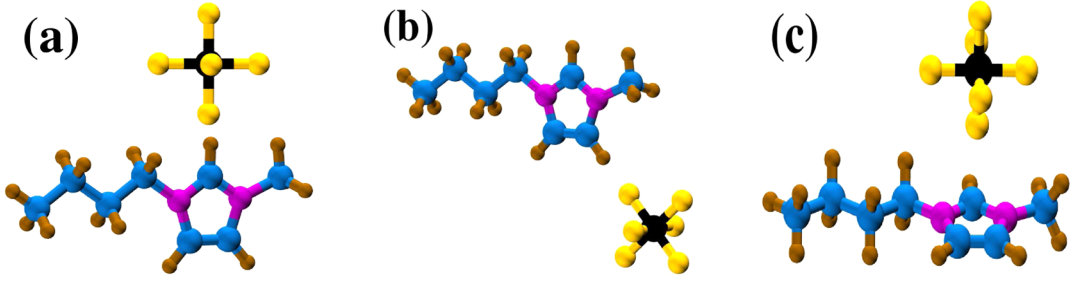

Figure 2. Directions along which the cation−anion distance was varied, shown here for [BMIM][PF_6]: (a) along the C−H_A bond; (b) along the C−H_B bond; (c) perpendicular to the imidazolium ring plane. Color scheme: nitrogen, purple; carbon, blue; hydrogen, ochre; phosphorus, black; fluorine, orange.

dx.doi.org/10.1021/jp500296x | J. Phys. Chem. B 2014, 118, 3409−3422

important in reproducing intermolecular structure accurately, which can have a bearing even on long time dynamics.[88] Here, the SR interactions between the particle types i and j are described through the standard 12-6 LJ potential with σ and ε as parameters.

Given that the site charges as well as the total ion charges are changed from values associated with the CLaP force field, one needs to adjust the parameters of both the nonbonded and dihedral interaction terms. Toward this purpose, we have carried out quantum chemical calculations of six different ion pairs in the gas phase with [BMIM] as a common cation. For each anion, these calculations involved three potential energy scan runs in each of which the cation−anion distance was varied along a certain direction. Such potential energy surfaces (PES) were taken as references against which those obtained using the refined force field were benchmarked. Nonbonded parameters (typically of sites in the anion) were refined so as to reproduce the PES of the quantum calculation. The latter were carried out using Gaussian09,[89] for which the initial structures were constructed using GaussView.[90] These reference calculations were calculated at M06/aug-cc-pvdz level of theory whose binding energy was within 2 kcal/mol of that obtained through MP2/aug-cc-pvdz level of theory. In the scan runs, the cation was held fixed while the anions were displaced along the (I) C_R−H_A vector, (II) C_W−H_B vector (closer to the methyl) and (III) perpendicular to the center of the imidazolium ring as illustrated in Figure 2a−c, respectively.

Scan runs with the same coordinates as used in the quantum run were initiated to obtain the PES from the empirical force field. These were carried out using LAMMPS.[86] In these gas phase scan runs alone, CLaP force field parameters were used to model the IL pairs with a unit ion charge value and with site charges as per CLaP. As these scan runs were conducted in the gas phase, the ions can be expected to be unaffected by polarization which is present in the condensed phase. Thus, the original site charges of CLaP were used. The box length was set to 200 Å in these calculations and the interaction sphere of a site included all other sites irrespective of distance. Nonbonded interaction parameters were iterated manually until the surfaces obtained from the force field best matched those from the quantum runs. To achieve this, the LJ parameters of the three hydrogen atoms directly attached to imidazolium ring (H_A and H_B) as well as of the sites on the anions were tuned. Parameters involving other atom types in the cation were unaltered from their CLaP values.

The first ion pair to be studied was [BMIM][PF_6] and the procedure described above was followed. However, while the LJ parameters of other anions were refined, the cation parameters were left unchanged and those of the sites on the anion alone were refined. Thus, in the refined force field, the LJ parameters of the cation are independent of cation tail length or of the anion type. The LJ parameters of the anion are independent of the cation tail length too. In Figure 3a−c, we show results of scan runs performed in case of [BMIM][PF_6]. In all the three directions, the potential well obtained from the CLaP model was seen to be marginally shallower and to be present at slightly larger distances relative to the quantum result. By refining the parameters, the location of the minimum in all the three scan runs for a given anion was obtained within 0.05 Å of the M06 result. The difference in the well depth between the quantum data and that of the refined force field was within 2.5 kcal/mol, for all the IL systems studied here. The tuned LJ potentials are provided in Table 1.

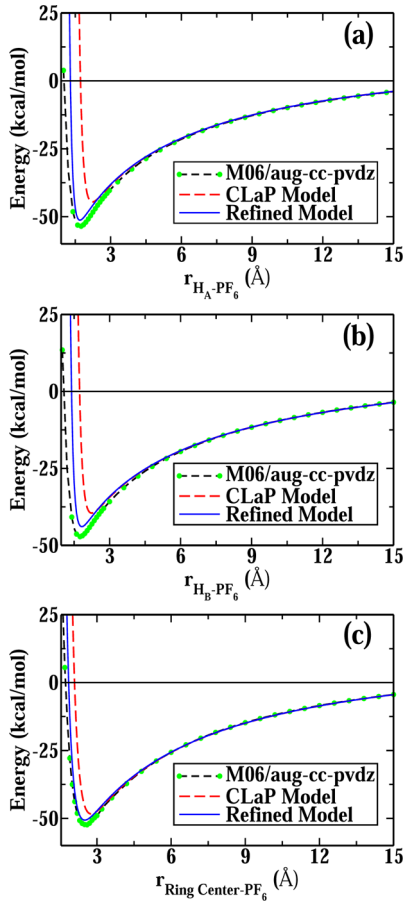

Figure 3. Potential energy as a function of distance between cation site and anion from quantum calculation (M06), from the CLaP model,[34−36] and from our refined model for [BMIM][PF_6]. The three directions are described Figure 2.

Dihedral Interactions. The 1−4 term (12-6 LJ and Coulomb with a scale factor) acts between atoms separated by three covalent bonds. Because the nonbonded interaction parameters have been altered, the 1−4 energy will also be changed. The effect of reparametrization of nonbonded interactions needs to be reflected in the 1−4 interactions as well, which will affect the dihedral energy too. Hence, the dihedral potential needs to be reparametrized. In this process, we found it convenient (within LAMMPS) to employ the multiharmonic function to describe the dihedral potential, expressed as,

$$E^{\text{MH}}_{\text{dihedral}} = \sum_{n=1}^{5} A_n \cos^{n-1}(\phi) \tag{1}$$

The dihedral interaction parameters A_i were refitted in a manner so as to reproduce the dihedral profile obtained from quantum chemical calculations. For the latter, we adopt the dihedral potential profile of the CLaP model. The procedure we follow is identical to that described in ref 72. The potential energy between sites 1 and 4 defined according to CLaP can be split as[72]

$$E^{\text{CLaP}} = E^{\text{CLaP}}_{1-4,\text{LJ}} + E^{\text{CLaP}}_{1-4,\text{Coulomb}} + E^{\text{CLaP}}_{\text{dihedral}} \tag{2}$$

Coulombic and LJ contributions to the 1−4 interactions in the CLaP model are scaled by a factor of 0.5. In our model, we employ this factor for 1−4 LJ interactions whereas that for 1−4

dx.doi.org/10.1021/jp500296x | J. Phys. Chem. B 2014, 118, 3409−3422

Table 1. Lennard-Jones Parameters for the 1-Alkyl-3-methylimidazolium Cation and Selected Anions According to the Refined Model[a]

atom	ε (kJ mol^{-1})	σ (Å)
N	0.71128	3.25
CR	0.29288	3.55
CW	0.29288	3.55
HA	0.04184	1.70
HB	0.12552	2.00
C1	0.27614	3.50
H1	0.12552	2.50
C2/CE	0.27614	3.50
HC	0.12552	2.50
CS	0.27614	3.50
CT	0.27614	3.50
P (PF_6^-)	0.83680	3.74
F (PF_6^-)	0.17152	2.75
B (BF_4^-)	0.25104	3.68
F (BF_4^-)	0.08368	2.80
N (NO_3^-)	0.33800	3.06
O (NO_3^-)	0.56816	2.70
S ($CF_3SO_3^-$)	0.75312	3.55
O ($CF_3SO_3^-$)	0.41840	2.80
C ($CF_3SO_3^-$)	0.15062	3.50
F ($CF_3SO_3^-$)	0.17991	2.95
N (NTf_2)	0.41840	3.25
S (NTf_2)	0.54392	3.55
O (NTf_2)	1.04600	2.96
C (NTf_2)	0.10878	3.50
F (NTf_2)	0.09623	2.95
Cl (Cl^-)	1.25452	3.30

[a]Atoms separated by three covalent bonds interact via 1−4 interactions with the following scale factors: 0.5 for Lennard-Jones and zero for Coulomb.

Coulomb interactions is zero (i.e., 1−4 pairs do not interact via Coulomb forces). This procedure aids in introducing better transferability to the force field. Note that the total 1−4 interaction energy in our force field for ions in gas phase is the same as that of the CLaP (eq 2). The dihedral energies in our refined model, E^{MH} can be obtained from

$$E^{\text{refined}} = E^{\text{refined}}_{1-4,\text{LJ}} + E^{\text{MH}}_{\text{dihedral}} = E^{\text{CLaP}} \quad (3)$$

We demand that E^{refined} be the same as E^{CLaP}. Thus,

$$E^{\text{refined}}_{1-4,\text{LJ}} + E^{\text{MH}}_{\text{dihedral}} = E^{\text{CLaP}}_{1-4,\text{LJ}} + E^{\text{CLaP}}_{1-4,\text{Coulomb}} + E^{CLaP}_{\text{dihedral}} \quad (4)$$

and

$$E^{\text{MH}}_{\text{dihedral}} = E^{\text{CLaP}}_{1-4,\text{LJ}} + E^{\text{CLaP}}_{1-4,\text{Coulomb}} + E^{\text{CLaP}}_{\text{dihedral}} - E^{\text{refined}}_{1-4,\text{LJ}} \quad (5)$$

To obtain the dihedral interaction parameters A_i, we have calculated the energies of every type of dihedral angle. Later, $E^{\text{MH}}_{\text{dihedral}}$ was fitted to eq 5. In this procedure, the positions of the first and last atoms of all the dihedral angles were stored with a step size of 5° over the range −180° to +180°. The OPLS potential was used to calculate $E^{\text{CLaP}}_{\text{dihedral}}$. The OPLS potential parameters for all the dihedral angles were taken from the CLaP model. At each step, the $E^{\text{MH}}_{\text{dihedral}}$ energy was calculated. The multiharmonic dihedral potential for two dihedral types, e.g., N−C_R−N−C_1 and C_R−N−C_1−C_2 are shown in Figure 4a,b, respectively, for purposes of illustration. From the first two plots, we can see that $E^{\text{CLaP}}_{\text{dihedral}}$ and $E^{\text{MH}}_{\text{dihedral}}$ are different. The E_{1-4} energies for those two dihedrals were also found to be different by about a few kcal/mol. Hence, it is evident that the reparametrization of short-range interactions does affect the dihedral potentials. Hence, it is important to adapt the dihedral potentials such that it would reproduce the dihedral energies obtained from quantum chemical calculations.

As discussed earlier, the LJ potential parameters for sites on the cation are independent of the IL that they constitute. Hence, in this dihedral refitting method, the set of LJ parameters used to calculate $E^{\text{refined}}_{1-4,\text{LJ}}$ are also the same for any IL. As $E^{\text{refined}}_{1-4,\text{Coulomb}}$ is chosen to be zero, the dihedral potential parameters for the cation too are independent of the specific IL. This characteristic imbues a general and transferable nature to the refined force field. Dihedral potentials for polyatomic anions containing dihedral angles, such as, bis-(trifluoromethylsulfonyl)imide (NTf_2) or triflate (CF_3SO_3), were also refined in a similar fashion. The dihedral interaction potentials for different types of dihedral angles are tabulated in Table 2. As an illustration, the energy profile of the dihedral angle term for the C−F−S−O bond in $CF_3SO_3^-$ anion is shown in the Supporting Information as Figure S2.

Molecular Dynamics Simulations. The refined set of force field parameters was used to model various ionic liquids. Classical molecular dynamics simulations of liquid phases of ILs were carried out in the isothermal−isobaric (*NPT*) as well as in canonical (*NVT*) ensembles using the LAMMPS[86] package. The particle−particle particle mesh Ewald (PPPM) solver was used to calculate the long-range interactions with a precision of 10^{-5}. Following the CLaP convention, real space cutoff distances were defined at 11, 12, and 13 Å for the $[EMIM]^+$, $[BMIM]^+$, and $[HMIM]^+$ salts, respectively. Long-range corrections to energy and pressure were applied. Equations of

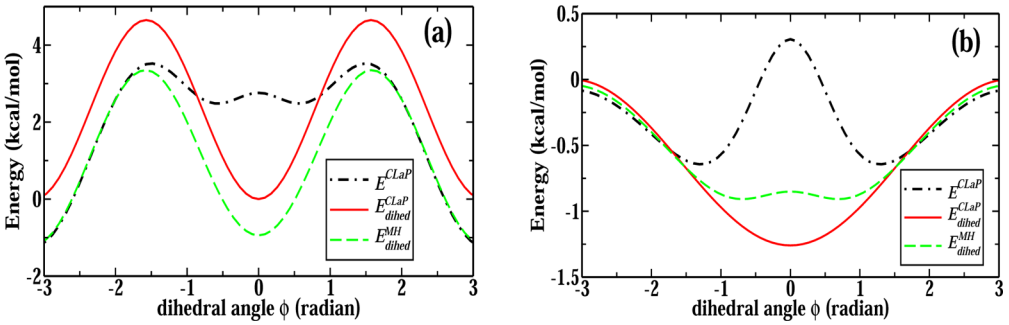

Figure 4. Energy profiles of the dihedral interaction for (a) N−C_R−N−C_1 and (b) C_R−N−C_1−C_2. Black (dash-dotted) line, E^{CLaP} is the reference energy between 1 and 4 sites. The green dashed line is $E^{\text{MH}}_{\text{dihedral}}$ derived using eq 5.

dx.doi.org/10.1021/jp500296x | J. Phys. Chem. B 2014, 118, 3409−3422

Table 2. Proper Dihedral Parameters in Multi/Harmonic Form According to the Refined Model: $E^{MH}_{dihedral} = \sum_{n=1}^{5} A_n \cos^{n-1}(\phi)$[a]

	A (kJ mol^{-1})				
dihedrals	A_1	A_2	A_3	A_4	A_5
N−C_R−N−C_W	14.7099	−0.95885	−19.7501	−0.11816	−0.04368
N−C_R−N−C_1	13.7712	−0.89994	−19.6735	−0.06280	−0.01782
N−C_W−C_W−N	50.4243	1.14629	−44.6186	0.15686	0.06079
N−C_W−C_W−H_B	52.7715	1.33905	−44.6014	3.97756	3.62251
N−C_1−C_2−H_C	2.27225	−0.21912	0.08213	0.75320	0.00109
N−C_1−C_2−C_S	−4.97220	−2.63207	−3.35502	−2.47295	−0.02335
C_R−N−C_1−H_1	−3.21080	−0.23108	0.08841	0.15008	0.08769
C_R−N−C_1−C_2	−2.86520	−2.66755	−0.00707	−0.00184	−0.00046
C_R−N−C_W−C_W	16.0210	0.69856	−12.3393	0.08548	0.03146
C_R−N−C_W−H_B	7.12874	−0.35581	−12.2003	0.74643	0.49777
C_W−N−C_R−H_A	13.0390	−0.40932	−19.0264	0.87567	0.57367
C_W−C_W−N−C_1	17.3763	0.74241	−12.3787	0.04866	0.01339
C_W−N−C_1−H_1	−3.53060	−1.10516	0.05991	1.17817	0.08523
C_W−N−C_1−C_2	2.66194	−4.80344	−6.11366	1.58603	−0.00042
H_B−C_W−N−C_1	4.77081	−0.77312	−12.6223	0.02983	0.02272
H_B−C_W−C_W−H_B	55.1903	0.74542	−44.8956	0.01226	0.00218
H_A−C_R−N−C_1	11.6353	−0.77517	−19.5152	0.05171	0.03464
C*−C*−C*−H*	−1.80660	−2.29693	0.00000	3.06260	0.00000
C*−C*−C*−C*	11.2836	1.88903	0.65689	2.33459	0.00000
H*−C*−C*−H*	1.59553	−1.86226	0.02908	2.66964	0.00197
		$[CF_3SO_3]^-$			
O−S−C−F	20.9362	1.17315	0.889769	3.46649	0.324511
		$[NTf_2]^-$			
N−S−C−F	21.8644	1.56059	0.96483	3.29636	0.38304
S−N−S−C	76.4973	33.7603	14.4047	−2.45383	2.57709
S−N−S−O	−109.112	−18.3380	−4.46968	−0.77684	0.13012
O−S−C−F	17.7697	0.66526	0.73270	3.25009	0.16869

[a]Improper dihedral parameters are the same as in the CLaP model.[34−36] C* represents a generic aliphatic carbon, C_1, C_2, C_E, C_S, or C_T. H* represents either H_1 or H_C.

motion were integrated using the velocity Verlet algorithm with a time step of 1 fs, while all the C−H covalent bonds were constrained. The temperature and pressure of the system were controlled by using the Nóse−Hoover thermostat[91] and barostat. In all the constant pressure simulations, pressure was held fixed at 1 atm. All systems were simulated at 300 K except [BMIM][Cl], which was studied at 353 K. Cubic periodic boundary conditions were applied.

Each ionic liquid was studied with 512 ion pairs. Initial molecular coordinates were set up using Packmol software.[92] The systems were equilibrated in the *NPT* ensemble for 10 ns. This was followed by production runs lasting 25 ns, generated in the *NVT* ensemble. All the systems are visualized using Mercury[93] and VMD.[94]

Surface tension was calculated using a simulation of the liquid−vapor interface. A pre-equilibrated configuration of the bulk liquid containing 512 molecules in the *NVT* ensemble was taken. The length of the simulation box along the *z*-axis was increased to 120 Å to generate two liquid−vacuum (or liquid−vapor) interfaces. A 10 ns trajectory was generated and the pressure tensor of the system was stored at every time step. The surface tension γ was calculated from the diagonal components of the pressure tensor P_{ii} using eq 6 at 300 K ([BMIM][Cl] at 353 K).

$$\gamma = \frac{l_z}{4}(2P_{zz} - P_{xx} - P_{yy}) \quad (6)$$

where l_z is the length of simulation box in the direction parallel to the interface normal, here the *z*- axis.

The crystalline phase of two ionic liquids, [BMIM][PF_6] and [BMIM][Cl] were also simulated using the refined set of force field parameters. Initial cell parameters and atom positions were taken from the experimentally determined crystal structures.[95,96] The size of the simulation cell considered for [BMIM][PF_6] and [BMIM][Cl] crystals was 4 × 4 × 4 and 3 × 3 × 4, respectively, consisting of 4096 and 3744 atoms. Classical molecular dynamics simulations were carried out in the fully flexible, isothermal−isobaric (*NPT*) ensemble at 173 and 200 K, respectively, using the LAMMPS[86] package. The ewald/n solver was used to calculate the long-range interactions with a precision of 10^{-5}. All other simulation protocols were the same as used in the simulation of liquid phases of ILs. The systems were equilibrated in the *NPT* ensemble for 3 ns and this was followed by production runs lasting 5 ns. Details of simulated cell parameters and their comparison with experiment are provided in Table S14 in the Supporting Information. The crystal structures were found to be stable in the simulations employing the refined force field.

RESULTS AND DISCUSSION

Atomic Charges. Charges calculated either from the crystal or from the corresponding liquid show a decrease in the total ion charge from unity, which accounts for the polarization and charge transfer effects in the bulk environment, as shown in Figure 5. The net ion charge varies from a value of ±0.64 e for the chloride to one of ±0.79 e for BF_4.

An interesting observation in the atomic charge distribution as well as in the total ion charges was noticed. Total ion charges

dx.doi.org/10.1021/jp500296x | J. Phys. Chem. B 2014, 118, 3409−3422

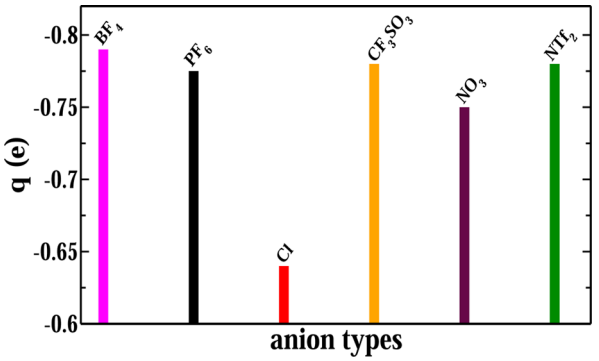

Figure 5. Ion charges of anions $[BF_4]^-$, $[PF_6]^-$, $[Cl]^-$, $[CF_3SO_3]^-$, $[NO_3]^-$, and $[NTf_2]^-$ in imidazolium based ILs obtained from their crystalline state.

calculated from the three crystalline compounds containing the same anion, [MMIM][PF_6], [EMIM][PF_6], and [BMIM][PF_6] ILs, were nearly identical. In this specific instance, these were found to be ±0.78, ± 0.77, and ±0.78 e, respectively. Similar behavior was observed in the atomic site charges for these ILs as well. Furthermore, atoms related to each other by crystal symmetry carried the same charge. In fact, this criterion was one of the vital ones that persuaded us to use the DDEC/c3 method over the ESP or Blöchl methods. Furthermore, nitrogen atoms present in the imidazolium ring of the above three ILs possess nearly the same charge values. Also, site charges on the cation were found to be comparable in ILs containing different anion types. The largest difference was for sites present on the imidazolium ring. In addition, it was observed that the charges of methyl or methylene groups lying beyond the second carbon atom (C_2) on the alkyl tail were quite small. Charges obtained by the DDEC/c3 method for all the crystals are provided in Table S3 to Table S13 in the Supporting Information. In the liquid phase, the charges on specific atoms in an IL too showed a spread of around 0.04e around respective mean values.

A comparison of the atomic charges obtained from the crystal and liquid phases was enlightening. As mentioned earlier, liquid phase atomic charges were calculated using a number of snapshots generated from classical MD simulation, which were subsequently optimized for their geometries (albeit to a coarse extent) within DFT. The ion charge distribution in the liquid phase of [BMIM][BF_4] and [BMIM][NO_3] are shown in Figure 6a,b, respectively. The ion charge from the crystal compares very well with the mean of the distribution from the liquid phase. Furthermore, the average charge values on every atomic site was found to be very close to atomic charges of the crystalline phase. Thus, for salts whose crystal structures have not been determined, one can employ this procedure to obtain the atomic site charges from the corresponding liquid. It is much less expensive than performing a full fledged AIMD simulation. The ion charge distribution in the liquid phase of few other ILs are shown in Figure S7 in the Supporting Information.

Our aim was to employ the same atom typing scheme of CLaP. To achieve a force field that is transferable across ILs, a few practical solutions were adopted. The site charges on the cation were revised keeping their total charges unchanged. First, for a particular type of anion, the total ion charges were taken to be the mean of ion charges of ILs containing this specific anion but with varying alkyl tail lengths on the imidazolium cation. Site charges of all different atom types were also averaged over in this fashion. Given that the total charge on the anions depended on their type, the charge on the imidazolium cation too would depend on the specific IL that it is present in. It is also desirable that the charges on the methylene group present beyond two bonds from the nitrogen of the ring are neutral; this will enable the use of the same atom types as that of CLaP. In an IL, the anions are located closer to the imidazolium ring than to the alkyl group of the cation. Thus, the total charge of methyl as well as methylene groups that are located beyond the $C_{2/E}$ carbon atom were changed to zero from the values calculated using DDEC/c3 method. The difference in the charges was distributed equally over all the sites on the imidazolium ring.

This procedure of a marginal reassignment of charges provides the advantage of having the same charge distribution within the alkyl part of the cation across all the ILs, independent of the anion type. Thus, the only difference in cation site charges in different ILs lies in the atoms of the imidazolium ring. Charges obtained through the DDEC/c3 method as applied to crystals as well as those recommended by us after reassignment for the sake of transferability are provided in Tables 3 and 4. These charges together with the nonbonded parameters provided in Table 1, constitute our refined force field.

In summary, the site charges on the imidazolium cation depend on the specific anion type that is present in the ionic liquid, as it would in a polarizable force field. However, the nonbonded, 1−4, and torsional parameters of the cation are independent of the anion type present in the IL.

Density. The liquid phase of seven IL systems were simulated using these refined set of partial charges combined with tuned LJ parameters and refitted dihedral interaction

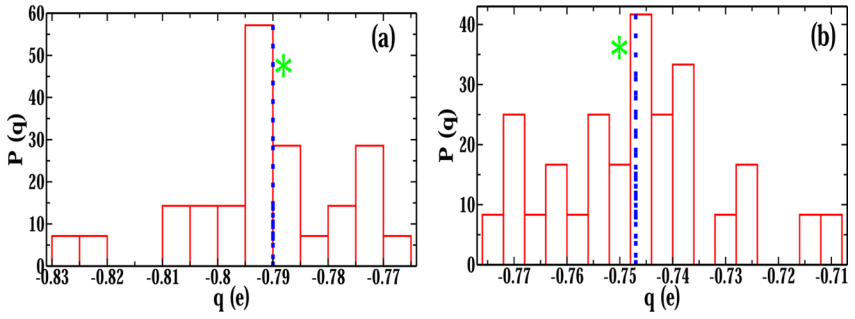

Figure 6. Distribution of ion charges calculated from snapshots of a MD simulation trajectory of liquid phase of (a) [BMIM][BF_4] and (b) [BMIM][NO_3]. The thin blue line is the mean of this distribution, and the star is the charge value in the crystalline phase.

dx.doi.org/10.1021/jp500296x | J. Phys. Chem. B 2014, 118, 3409−3422

Table 3. Atomic Site Charges (e) for the Cation According to the Refined Model

atom type	$[PF_6]^-$	$[BF_4]^-$	$[NO_3]^-$	$[CF_3SO_3]^-$	$[Cl]^-$	$[NTf_2]^-$
N	0.145	0.140	0.145	0.145	0.130	0.145
CR	−0.005	−0.010	−0.005	−0.030	−0.010	−0.005
CW	−0.110	−0.110	−0.120	−0.110	−0.130	−0.120
HA	0.170	0.180	0.165	0.180	0.150	0.175
HB	0.160	0.170	0.160	0.170	0.140	0.170
C1	−0.250	−0.250	−0.250	−0.250	−0.250	−0.250
H1	0.120	0.120	0.120	0.120	0.120	0.120
C2	−0.076	−0.076	−0.076	−0.076	−0.076	−0.076
CE	−0.174	−0.174	−0.174	−0.174	−0.174	−0.174
HC	0.098	0.098	0.098	0.098	0.098	0.098
CS	−0.196	−0.196	−0.196	−0.196	−0.196	−0.196
CT	−0.294	−0.294	−0.294	−0.294	−0.294	−0.294

Table 4. Atomic Site Charges (e) for the Anion According to the Refined Model

atom	charge
P (PF_6^-)	1.589
F (PF_6^-)	−0.394
B (BF_4^-)	1.010
F (BF_4^-)	−0.450
N (NO_3^-)	0.780
O (NO_3^-)	−0.510
S ($CF_3SO_3^-$)	1.090
O ($CF_3SO_3^-$)	−0.600
C ($CF_3SO_3^-$)	0.440
F ($CF_3SO_3^-$)	−0.170
N (NTf_2)	−0.740
S (NTf_2)	1.090
O (NTf_2)	−0.545
C (NTf_2)	0.445
F (NTf_2)	−0.155
Cl (Cl^-)	−0.640

potentials. These systems were [BMIM][BF_4], [BMIM][PF_6], [HMIM][PF_6], [BMIM][CF_3SO_3], [BMIM][Cl], [BMIM]-[NO_3], and [BMIM][NTf_2]. All of them were studied at 300 K, except for [BMIM][Cl], which was studied at 353 K due to its higher melting point.

The liquid phase densities of all the IL systems were calculated from MD simulations performed in the constant-temperature constant-pressure (*NPT*) ensemble. The computed densities are within 2% of experimental results (Table 5) and are compared in Figure 7. The CLaP model has been documented to reproduce liquid phase density well.[48] However,

Table 5. Liquid Phase Densities (g/cm^3) of ILs Obtained from Simulations Using the Refined Force Field Compared with Experimental Data at 300 K[a]

system	ρ_{exp}	ρ_{sim}	$\Delta\rho$ (%)
[BMIM][BF_4]	1.202[97]	1.206	+0.33
[BMIM][PF_6]	1.368[97]	1.388	+1.31
[HMIM][PF_6]	1.293[98]	1.310	+1.31
[BMIM][NO_3]	1.154[99]	1.164	+0.86
[BMIM][CF_3SO_3]	1.298[97]	1.317	+1.45
[BMIM][NTf_2]	1.437[97]	1.446	+0.62
[BMIM][Cl][b]	1.050[100]	1.038	−1.14

[a]The uncertainty in the simulated density is around 0.002 g/cm^3. [b]The temperature is 348 K.

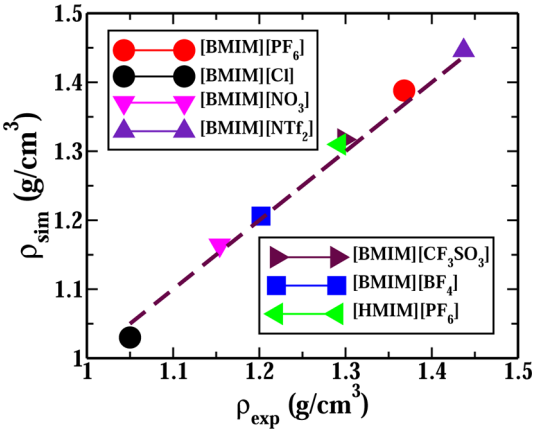

Figure 7. Scatter plot of liquid phase densities of ionic liquids: comparison between experiment and simulation. The dashed line is the target.

an earlier attempt to employ partial charges (obtained from the crystalline phase) for liquid [BMIM][PF_6] and [EMIM][PF_6][74] yielded differences in density of around 6%. This example shows the importance of refining the nonbonded and torsional interaction parameters along with the site charges.

Heat of Vaporization. Vaporization enthalpy is an important physical property that is a signature of the strength of intermolecular interactions. The strong electrostatic interaction between the ions is a major reason for the higher heat of vaporization of ionic liquids relative to those of molecular liquids. Heats of vaporization (ΔH_{vap}) can be computed from simulations using the following eq 7.

$$\Delta H_{vap} = \Delta H_{gas} - \Delta H_{liquid} = E_{total}^{gas} - E_{total}^{liquid} + RT \quad (7)$$

E_{total}^{gas} is the average potential energy for an ion pair in the gas phase and E_{total}^{liquid} is the corresponding value in the liquid phase. The vaporization enthalpy was computed for all these IL systems parametrized by the refined force field and the results are summarized in Table 6. It is very difficult to compare the computed and experimental heats of vaporization values as the values reported using different experimental techniques differ from each other significantly.[101,102] It is evident that the values obtained from simulations show satisfactory agreement with experimental results. Experimental ΔH_{vap} values for [BMIM]-[Cl] are not available, but our estimates compare well with the value of 29.1 kcal/mol obtained by simulations earlier.[43] Table 6 also displays values of vaporization enthalpy reported by other simulations in the literature (ΔH_{vap}).

dx.doi.org/10.1021/jp500296x | J. Phys. Chem. B 2014, 118, 3409−3422

Table 6. Heat of Vaporization (kcal/mol) at 300 K of ILs Obtained from Simulations Compared against Experimental Data at 298 K[a]

system	ΔH_{vap}^{exp}	ΔH_{vap}^{sim}	error (%)	$\Delta H_{vap}^{lit.}$
[BMIM][BF_4]	33.78[103]	31.90	−5.56	27.8,[43] 33.6[104]
[BMIM][PF_6]	37.00[105]	33.00	−10.81	31.9,[43] 35.9[104]
[HMIM][PF_6]	33.41[106]	34.70	+3.86	40.1[43]
[BMIM][NO_3]	37.52[107]	33.57	−10.52	36.2[104]
[BMIM][CF_3SO_3]	33.22[108]	32.94	−0.84	31.1,[43] 34.1[104]
[BMIM][NTf_2]	32.17[106]	31.23	−2.92	31.9[104]
[BMIM][Cl][b]		28.02		29.1[43]

[a]The estimated standard error on the mean in the simulated heat of vaporization is around 0.02 kcal/mol. [b]The temperature is 353 K.

Radial Distribution Functions. Radial distribution functions (RDFs) of anion around cation and of anion around the acidic proton (H_A) were obtained from the refined model, and a few of them are shown in Figure 8. The RDFs between the geometric centers of the imidazolium ring and the central atom of the corresponding anion are shown in Figure 8a. Figure 8b exhibits the same between the central atom of the anion and the acidic proton of the cation. Results of other radial distribution functions are provided in Figure S3 and Figure S4 in Electronic Supporting Information.

For all the ionic liquids, the cation−anion RDFs show a well structured first peak and a shoulder between 5 and 7 Å. Such features have been observed and discussed in earlier simulations.[49,39] These effects are due to charge ordering[109] and van der Waals interactions and are observed up to a distance of 20 Å (data shown in the Supporting Information). In earlier reports, it was found that the anion prefers to locate itself around the acidic hydrogen (H_A), rather than near H_B or H sites present in the methyl (H_1) or alkyl group (H_C).[39] Moreover, such an arrangement leads to the formation of a hydrogen bond between the acidic hydrogen and the anion. The anion-H_A(C_R) RDF obtained from the refined model is able to well reproduce this important feature. The RDF of H_A−Cl in [BMIM][Cl] shows the highest peak among all ILs and $[BF_4]^-$ anion was found to have interact strongly with H_A than $[PF_6]^-$ or $[NO_3]^-$ does. These observations are in good agreement with earlier results.[39,110]

Spatial Distribution Functions. Spatial distribution functions (SDFs) were used for further characterization of intermolecular structure in the liquid. The spatial density map of anion around the cation center of mass are shown in Figure 9. The isosurface value of the anion density presented in all the figures is 0.021 $Å^{-3}$.

Anions have three preferred binding sites around the cation. These are positioned around the three ring hydrogens: one H_A and two H_B atoms. Among these three, the most preferred one is the former. Anions are also present above and below the ring plane. Between the two H_B atoms, anions favor the methyl side rather than the butyl (alkyl) side, as the conformational flexibility of the latter can cause steric hindrance to the anion.

Surface Tension. The calculated values of surface tension are compared against experimental data in Table 7 and the agreement is quite reasonable (Figure 10).

Mean Square Displacement and Self-Diffusion Coefficients. Transport properties of ionic liquids were determined from a calculation of mean square displacement (MSD) of the center of mass of ions. MSD was calculated for the ILs at 300 K (except for [BMIM][Cl] at 353 K) on the basis of a 25 ns *NVT* trajectory and are shown in Figure S5 in the Supporting Information. Consistent with experiments[112,113] and many simulations,[49,55,114] the cations diffuse faster than anions.

To check whether the system is in the diffusive regime, we have calculated the exponent $\beta(t)$, defined as

$$\beta(t) = \frac{\mathrm{d}\ln\langle \Delta r^2(t)\rangle}{\mathrm{d}\ln(t)} \tag{8}$$

where $\Delta r^2(t)$ is the mean square displacement at time *t*. $\beta(t) < 1$ implies that the dynamics of the system is subdiffusive, whereas $\beta(t) = 1$ implies diffusive motion. $\beta(t)$ values for each ion type were computed as a function of time, and these are shown in Figure S6 in the Supporting Information. The self-diffusion coefficients were obtained from the slope of the mean square displacement data for the ions in the diffusive regime. The time window over which the slope was calculated for each system are provided in Table S15 in the Supporting Information. The calculated values of self-diffusion coefficients are given in Table 8. The values reported here shows a significant increase in the ion dynamics over the CLaP force field and are within 20% of experimental results in many systems.

CONCLUSIONS

Periodic density functional theory calculations have been carried out for crystalline and liquid phases of various room temperature ionic liquids. The electronic charge density obtained from such calculations have been used to determine site charges on atoms through the robust DDEC/c3[75,76] method. Atomic site charges were obtained from both these phases for ILs containing six different anion types, hexafluorophosphate (PF_6), tetrafluoroborate (BF_4), bis-

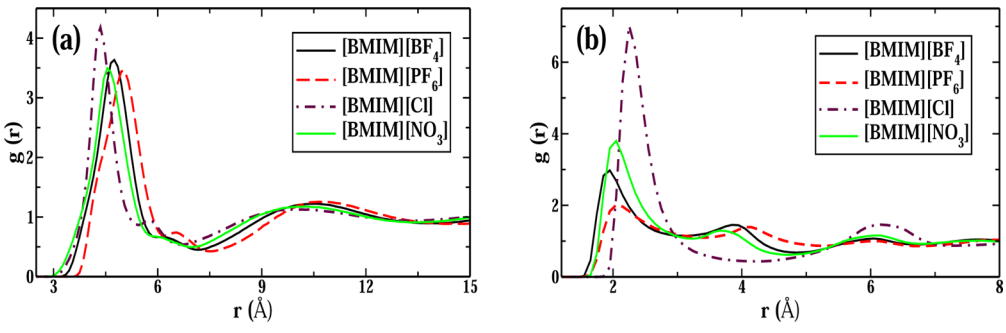

Figure 8. Radial distribution functions for (a) cation−anion and (b) anion−H_A for four ionic liquids obtained using the refined model.

dx.doi.org/10.1021/jp500296x | J. Phys. Chem. B 2014, 118, 3409−3422

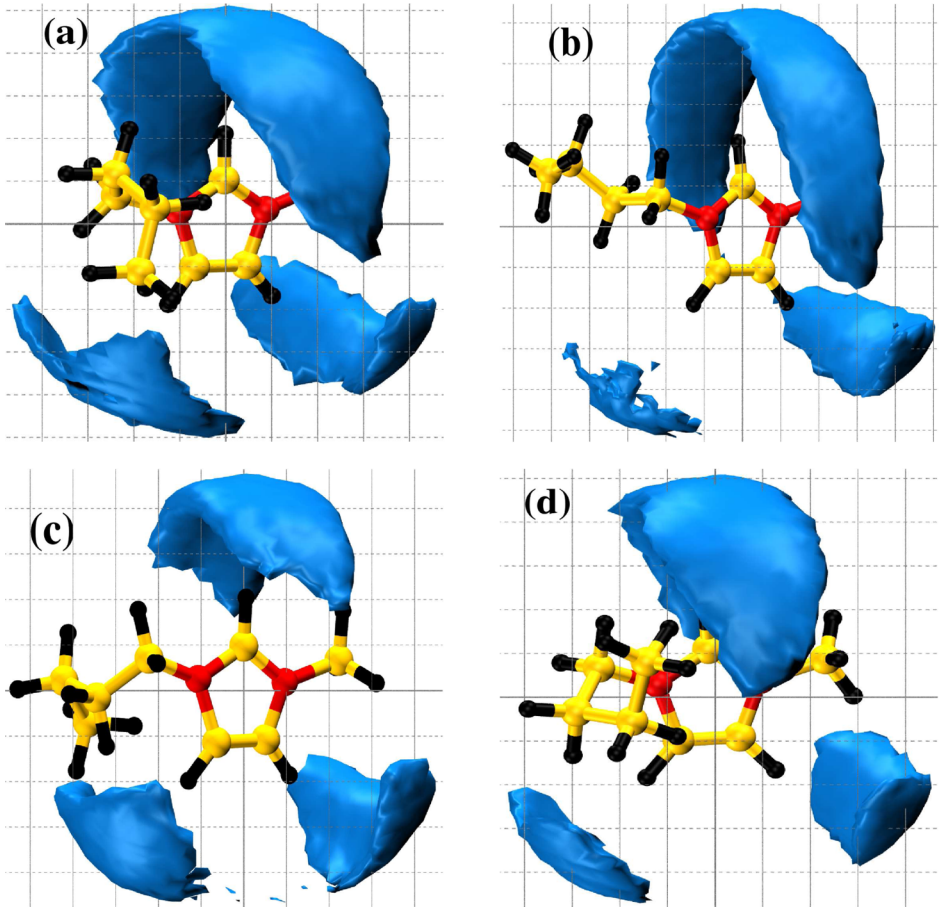

Figure 9. Spatial distribution function of anions around the cation at an isosurface value of 0.021 $Å^{-3}$: (a) [BMIM][BF_4]; (b) [BMIM][PF_6]; (c) [BMIM][Cl]; (d) [BMIM][NO_3]. Color scheme: red, nitrogen; orange, carbon; black, hydrogen.

Table 7. Surface Tension (mN/m) of ILs at 300 K Calculated Using the Refined Force Field Compared with Experimental Results[a]

system	γ_{exp}	γ_{sim}	error (%)
[BMIM][BF_4]	44.18 ± 0.02[111]	40.85	−7.5
[BMIM][PF_6]	43.52 ± 0.04[111]	47.10	8.2
[HMIM][PF_6]	38.35 ± 0.02[111]	40.21	4.5
[BMIM][NO_3]		51.20	
[BMIM][CF_3SO_3]	35.05 ± 0.03[111]	31.65	−4.2
[BMIM][NTf_2]	33.09 ± 0.02[111]	36.15	9.1
[BMIM][Cl][b]		39.52	

[a]The uncertainty in the calculated surface tension is around 0.06 mN/m. [b]The temperature is 353 K.

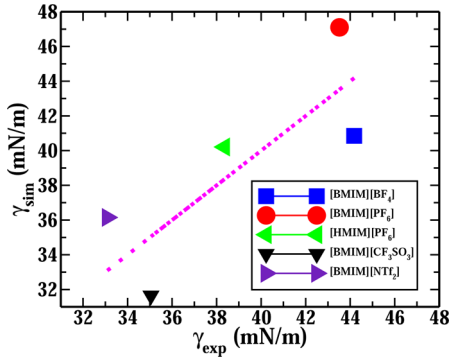

Figure 10. Scatter plot for the comparison of surface tension of ionic liquids between experiment and simulations. The dashed line is the target.

(trifluoromethylsulfonyl)imides (NTf_2), chloride (Cl), nitrate (NO_3), and trifluoromethanesulfonate or triflate (CF_3SO_3). The set of partial charges are crucial in the refinement of the force field, as electrostatic interactions are dominant in these liquids. The total ion charges obtained through this procedure were less than unity, which captures the effect of polarization and charge transfer from neighboring ions in the bulk environment. Surprisingly, for the five molecular anions studied here, the total ion charge varied over a narrow range, from 0.75 to 0.8 e. The charge on the chloride as obtained from crystalline [BMIM][Cl] was −0.6 e, implying the greater extent of charge transfer in this system due to its relatively smaller size.

Although the charges obtained here are from crystals, we have demonstrated that the mean ion charge in the liquid state is nearly the same as that obtained from the crystal. Further, the ion charge distribution in the liquid is rather narrow as well. This observation offers the possibility of charge determination by first carrying out a MD simulation of the desired liquid using a reasonable force field followed by coarse geometry optimizations within DFT of a few snapshots derived therefrom. The procedure to obtain site charges either from the crystal or from the liquid is quite tractable. These procedures are much less expensive than performing a full-blown ab initio MD simulation and are thus attractive.

dx.doi.org/10.1021/jp500296x | J. Phys. Chem. B 2014, 118, 3409−3422

Table 8. Self-Diffusion Coefficients of Ions in Various Ionic Liquids at 300 K Calculated Using the Refined Force Field Compared against Experimental Values Reported at 303 K[a]

	D_+ ($\times 10^{-7}$ cm^2 s^{-1})		ΔD_+ (%)	D_- ($\times 10^{-7}$ cm^2 s^{-1})		ΔD_- (%)
system	exp	sim		exp	sim	
[BMIM][BF_4]	1.80[97]	2.30	27.7	1.70[97]	1.83	7.6
[BMIM][PF_6]	0.89[97]	1.05	17.9	0.71[97]	0.74	4.2
[HMIM][PF_6]		0.54			0.47	
[BMIM][NO_3]		1.65			1.51	
[BMIM][CF_3SO_3]	2.10[97]	2.08	−0.95	1.60[97]	1.41	−11.8
[BMIM][NTf_2]	3.40[97]	2.70	−20.5	2.60[97]	2.10	−19.2
[BMIM][Cl][b]		14.1			17.3	

[a]The uncertainty in the calculated values is around 0.02 × 10^{-7} cm^2 s^{-1}. [b]The temperature is 353 K.

A transferable force field for ionic liquids was derived using these set of partial charges as a basis. We adapted the well established CLaP force field for this purpose; its nonbonded, 1−4, and torsional parameters were refined. This refinement procedure was carried out by using three potential energy surfaces established by gas phase quantum chemical calculations of ion pairs, as benchmarks.

With the combination of refined site charges obtained from condensed phase DFT calculations and the fine-tuned nonbonded and torsional parameters, classical MD simulations of various ionic liquids were carried out. The calculated physical properties (density, heat of vaporization, surface tension, diffusion coefficients) are in nearly quantitative agreement with experimental data.

In principle, this procedure can be extended to other imidazolium based ionic liquids with other anion types, as well as to pyridinium or amino acid based salts. These form our objective for the near future.

■ ASSOCIATED CONTENT

Supporting Information

Summary of cell parameters of different crystalline systems, information about the liquid systems studied for charge calculation, description of other methods that have been used for charge calculation, atomic site charges for different ILs, energy profile of the 1−4 interaction for different dihedral types, simulated cell parameters studied using refined model, the time window over which the slope of MSD was calculated to obtain diffusion coefficients and distribution of ion charges obtained from liquid simulations, site−site radial distribution functions, mean squared displacements of ILs, calculated $\beta(t)$ values for ionic liquids, and ion charge distributions. This material is available free of charge via the Internet at http://pubs.acs.org.

■ AUTHOR INFORMATION

Corresponding Author

*S. Balasubramanian: e-mail, bala@jncasr.ac.in.

Notes

The authors declare no competing financial interest.

■ ACKNOWLEDGMENTS

The genesis of this work lies in a question that Prof. Christian Holm asked Dr. Yong Zhang during the latter's presentation of work discussed in ref 74 at the March 2012 meeting of the American Chemical Society. S.B. acknowledges the question and the discussion which followed. We thank DST for support. S.B. thanks Sheikh Saqr Laboratory, JNCASR, for a senior fellowship. We thank the Centre for the Development of Advanced Computing, Bangalore, and CSIR-4PI, Bangalore, where a part of the computations were carried out.

■ REFERENCES

(1) Dupont, J. From Molten Salts to Ionic Liquids: A "Nano" Journey. *Acc. Chem. Res.* **2011**, *44*, 1223−1231.

(2) Ma, Z.; Yu, J.; Dai, S. Preparation of Inorganic Materials Using Ionic Liquids. *Adv. Mater.* **2010**, *22*, 261−285.

(3) Maginn, E. J. Atomistic Simulation of the Thermodynamic and Transport Properties of Ionic Liquids. *Acc. Chem. Res.* **2007**, *40*, 1200−1207.

(4) Maginn, E. J. Molecular Simulation of Ionic Liquids: Current Status and Future Opportunities. *J. Phys.: Condens. Matter* **2009**, *21*, 373101.

(5) Anderson, J. L.; Dixon, J. K.; Brennecke, J. F. Solubility of CO_2, CH_4, C_2H_6, C_2H_4, O_2, and N_2 in 1-Hexyl-3-methylpyridinium Bis(trifluoromethylsulfonyl)imide: Comparison to Other Ionic Liquids. *Acc. Chem. Res.* **2007**, *40*, 1208−1216.

(6) Wang, Y.; Jiang, W.; Yan, T.; Voth, G. A. Understanding Ionic Liquids through Atomistic and Coarse-Grained Molecular Dynamics Simulations. *Acc. Chem. Res.* **2007**, *40*, 1193−1199.

(7) Krekeler, C.; Dommert, F.; Schmidt, J.; Zhao, Y. Y.; Holm, C.; Berger, R.; Delle Site, L. Electrostatic Properties of Liquid 1,3-dimethylimidazolium chloride: Role of Local Polarization and Effect of the Bulk. *Phys. Chem. Chem. Phys.* **2010**, *12*, 1817−1821.

(8) Schröder, C. Comparing Reduced Partial Charge Models with Polarizable Simulations of Ionic Liquids. *Phys. Chem. Chem. Phys.* **2012**, *14*, 3089−3102.

(9) Fumino, K.; Wulf, A.; Ludwig, R. Strong, Localized, and Directional Hydrogen Bonds Fluidize Ionic Liquids. *Angew. Chem., Int. Ed.* **2008**, *47*, 8731−8734.

(10) Brennecke, J. F.; Gurkan, B. E. Ionic Liquids for CO_2 Capture and Emission Reduction. *J. Phys. Chem. Lett.* **2010**, *1*, 3459−3464.

(11) Gurkan, B.; Goodrich, B. F.; Mindrup, E. M.; Ficke, L. E.; Massel, M.; Seo, S.; Senftle, T. P.; Wu, H.; Glaser, M. F.; Shah, J. K.; Maginn, E. J.; Brennecke, J. F.; Schneider, W. F. Molecular Design of High Capacity, Low Viscosity, Chemically Tunable Ionic Liquids for CO_2 Capture. *J. Phys. Chem. Lett.* **2010**, *1*, 3494−3499.

(12) Niedermeyer, H.; Hallett, J. P.; Villar-Garcia, I. J.; Hunt, P. A.; Welton, T. Mixtures of Ionic Liquids. *Chem. Soc. Rev.* **2012**, *41*, 7780−7802.

(13) Hallett, J. P.; Welton, T. Room-Temperature Ionic Liquids: Solvents for Synthesis and Catalysis. 2. *Chem. Rev.* **2011**, *111*, 3508−3576.

(14) Wishart, J. F. Energy Applications of Ionic Liquids. *Energy Environ. Sci.* **2009**, *2*, 956−961.

(15) Jin, H.; O'Hare, B.; Dong, J.; Arzhantsev, S.; Baker, G. A.; Wishart, J. F.; Benesi, A. J.; Maroncelli, M. Physical Properties of Ionic Liquids Consisting of the 1-Butyl-3-Methylimidazolium Cation with Various Anions and the Bis(trifluoromethylsulfonyl)imide Anion with Various Cations. *J. Phys. Chem. B* **2008**, *112*, 81−92.

(16) Liu, H.; Maginn, E.; Visser, A. E.; Bridges, N. J.; Fox, E. B. Thermal and Transport Properties of Six Ionic Liquids: An Experimental and Molecular Dynamics Study. *Ind. Eng. Chem. Res.* **2012**, *51*, 7242−7254.

(17) Del Pópolo, M. G.; Lynden-Bell, R. M.; Kohanoff, J. Ab Initio Molecular Dynamics Simulation of a Room Temperature Ionic Liquid. *J. Phys. Chem. B* **2005**, *109*, 5895−5902.

(18) Bühl, M.; Chaumont, A.; Schurhammer, R.; Wipff, G. Ab Initio Molecular Dynamics of Liquid 1,3-Dimethylimidazolium Chloride. *J. Phys. Chem. B* **2005**, *109*, 18591−18599.
(19) Bhargava, B.; Balasubramanian, S. Intermolecular Structure and Dynamics in an Ionic Liquid: A Car-Parrinello Molecular Dynamics Simulation Study of 1,3-dimethylimidazolium chloride. *Chem. Phys. Lett.* **2006**, *417*, 486−491.
(20) Bagno, A.; D'Amico, F.; Saielli, G. Computing the 1H NMR Spectrum of a Bulk Ionic Liquid from Snapshots of Car-Parrinello Molecular Dynamics Simulations. *ChemPhysChem* **2007**, *8*, 873−881.
(21) Spickermann, C.; Thar, J.; Lehmann, S. B. C.; Zahn, S.; Hunger, J.; Buchner, R.; Hunt, P. A.; Welton, T.; Kirchner, B. Why are Ionic Liquid Ions Mainly Associated in Water? A Car-Parrinello Study of 1-ethyl-3-methyl-imidazolium chloride Water Mixture. *J. Chem. Phys.* **2008**, *129*, 104505.
(22) Kirchner, B.; Seitsonen, A. P. Ionic Liquids from Car-Parrinello Simulations. 2. Structural Diffusion Leading to Large Anions in Chloraluminate Ionic Liquids. *Inorg. Chem.* **2007**, *46*, 2751−2754.
(23) Thar, J.; Brehm, M.; Seitsonen, A. P.; Kirchner, B. Unexpected Hydrogen Bond Dynamics in Imidazolium-Based Ionic Liquids. *J. Phys. Chem. B* **2009**, *113*, 15129−15132.
(24) Mallik, B. S.; Siepmann, J. I. Thermodynamic, Structural and Transport Properties of Tetramethyl Ammonium Fluoride: First Principles Molecular Dynamics Simulations of an Unusual Ionic Liquid. *J. Phys. Chem. B* **2010**, *114*, 12577−12584.
(25) Zahn, S.; Wendler, K.; Delle Site, L.; Kirchner, B. Depolarization of Water in Protic Ionic Liquids. *Phys. Chem. Chem. Phys.* **2011**, *13*, 15083−15093.
(26) Yan, T.; Burnham, C. J.; Del Pópolo, M. G.; Voth, G. A. Molecular Dynamics Simulation of Ionic Liquids: The Effect of Electronic Polarizability. *J. Phys. Chem. B* **2004**, *108*, 11877−11881.
(27) Yan, T.; Wang, Y.; Knox, C. On the Structure of Ionic Liquids: Comparisons between Electronically Polarizable and Nonpolarizable Models I. *J. Phys. Chem. B* **2010**, *114*, 6905−6921.
(28) Borodin, O. Polarizable Force Field Development and Molecular Dynamics Simulations of Ionic Liquids. *J. Phys. Chem. B* **2009**, *113*, 11463−11478.
(29) Schröder, C.; Steinhauser, O. Simulating Polarizable Molecular Ionic Liquids with Drude Oscillators. *J. Chem. Phys.* **2010**, *133*, 154511.
(30) Zhao, W.; Leroy, F.; Heggen, B.; Zahn, S.; Kirchner, B.; Balasubramanian, S.; Müller-Plathe, F. Are There Stable Ion-Pairs in Room-Temperature Ionic Liquids? Molecular Dynamics Simulations of 1-n-Butyl-3-methylimidazolium Hexafluorophosphate. *J. Am. Chem. Soc.* **2009**, *131*, 15825−15833.
(31) Tsuzuki, S.; Matsumoto, H.; Shinoda, W.; Mikami, M. Effects of Conformational Flexibility of Alkyl Chains of Cations on Diffusion of Ions in Ionic Liquids. *Phys. Chem. Chem. Phys.* **2011**, *13*, 5987−5993.
(32) Pensado, A. S.; Gomes, M. F. C.; Lopes, J. N. C.; Malfreyt, P.; Pádua, A. A. H. Effect of Alkyl Chain Length and Hydroxyl Group Functionalization on the Surface Properties of Imidazolium Ionic Liquids. *Phys. Chem. Chem. Phys.* **2011**, *13*, 13518−13526.
(33) Lynden-Bell, R. M.; Atamas, N. A.; Vasilyuk, A.; Hanke, C. G. Chemical Potentials of Water and Organic Solutes in Imidazolium Ionic Liquids: a Simulation Study. *Mol. Phys.* **2002**, *100*, 3225−3229.
(34) Canongia Lopes, J. N.; Deschamps, J.; Pádua, A. A. H. Modeling Ionic Liquids Using a Systematic All-Atom Force Field. *J. Phys. Chem. B* **2004**, *108*, 2038−2047.
(35) Canongia Lopes, J. N.; Deschamps, J.; Pádua, A. A. H. Modeling Ionic Liquids Using a Systematic All-Atom Force Field. *J. Phys. Chem. B* **2004**, *108*, 11250−11250.
(36) Canongia Lopes, J. N.; Pádua, A. A. H. Molecular Force Field for Ionic Liquids Composed of Triflate or Bistriflylimide Anions. *J. Phys. Chem. B* **2004**, *108*, 16893−16898.
(37) Canongia Lopes, J. N.; Pádua, A. A. H. Molecular Force Field for Ionic Liquids III: Imidazolium, Pyridinium, and Phosphonium Cations; Chloride, Bromide, and Dicyanamide Anions. *J. Phys. Chem. B* **2006**, *110*, 19586−19592.
(38) Canongia Lopes, J. N.; Pádua, A. A. H.; Shimizu, K. Molecular Force Field for Ionic Liquids IV: Trialkylimidazolium and Alkoxycarbonyl-Imidazolium Cations; Alkylsulfonate and Alkylsulfate Anions. *J. Phys. Chem. B* **2008**, *112*, 5039−5046.
(39) Liu, Z.; Huang, S.; Wang, W. A Refined Force Field for Molecular Simulation of Imidazolium-Based Ionic Liquids. *J. Phys. Chem. B* **2004**, *108*, 12978−12989.
(40) Liu, Z.; Chen, T.; Bell, A.; Smit, B. Improved United-Atom Force Field for 1-Alkyl-3-methylimidazolium Chloride. *J. Phys. Chem. B* **2010**, *114*, 4572−4582.
(41) Liu, Z.; Chen, T.; Bell, A. T.; Smit, B. Improved United-Atom Force Field for 1-Alkyl-3-methylimidazolium Chloride. *J. Phys. Chem. B* **2010**, *114*, 10692−10692.
(42) Zhong, X.; Liu, Z.; Cao, D. Improved Classical United-Atom Force Field for Imidazolium-Based Ionic Liquids: Tetrafluoroborate, Hexafluorophosphate, Methylsulfate, Trifluoromethylsulfonate, Acetate, Trifluoroacetate, and Bis(trifluoromethylsulfonyl)amide. *J. Phys. Chem. B* **2011**, *115*, 10027−10040.
(43) Sambasivarao, S. V.; Acevedo, O. Development of OPLS-AA Force Field Parameters for 68 Unique Ionic Liquids. *J. Chem. Theory Comput.* **2009**, *5*, 1038−1050.
(44) Wang, Y.; Izvekov, S.; Yan, T.; Voth, G. A. Multiscale Coarse-Graining of Ionic Liquids. *J. Phys. Chem. B* **2006**, *110*, 3564−3575.
(45) Bhargava, B. L.; Balasubramanian, S.; Klein, M. L. Modelling Room Temperature Ionic Liquids. *Chem. Commun.* **2008**, 3339−3351.
(46) Roy, D.; Maroncelli, M. An Improved Four-Site Ionic Liquid Model. *J. Phys. Chem. B* **2010**, *114*, 12629−12631.
(47) Qiao, B.; Krekeler, C.; Berger, R.; Delle Site, L.; Holm, C. Effect of Anions on Static Orientational Correlations, Hydrogen Bonds, and Dynamics in Ionic Liquids: A Simulational Study. *J. Phys. Chem. B* **2008**, *112*, 1743−1751.
(48) Dommert, F.; Schmidt, J.; Qiao, B.; Zhao, Y.; Krekeler, C.; Delle Site, L.; Berger, R.; Holm, C. A Comparative Study of Two Classical Force Fields on Statics and Dynamics of [EMIM][BF_4] Investigated Via Molecular Dynamics Simulations. *J. Chem. Phys.* **2008**, *129*, 224501.
(49) Bhargava, B. L.; Balasubramanian, S. Refined Potential Model for Atomistic Simulations of Ionic Liquid [bmim][PF_6]. *J. Chem. Phys.* **2007**, *127*, 114510.
(50) Köddermann, T.; Paschek, D.; Ludwig, R. Molecular Dynamic Simulations of Ionic Liquids: A Reliable Description of Structure, Thermodynamics and Dynamics. *ChemPhysChem* **2007**, *8*, 2464−2470.
(51) Cadena, C.; Zhao, Q.; Snurr, R. Q.; Maginn, E. J. Molecular Modeling and Experimental Studies of the Thermodynamic and Transport Properties of Pyridinium-Based Ionic Liquids. *J. Phys. Chem. B* **2006**, *110*, 2821−2832.
(52) Santos, L. M. N. B. F.; Canongia Lopes, J. N.; Coutinho, J. A. P.; Esperança, J. M. S. S.; Gomes, L. R.; Marrucho, I. M.; Rebelo, L. P. N. Ionic Liquids: First Direct Determination of their Cohesive Energy. *J. Am. Chem. Soc.* **2007**, *129*, 284−285.
(53) Tokuda, H.; Hayamizu, K.; Ishii, K.; Susan, M. A. B. H.; Watanabe, M. Physicochemical Properties and Structures of Room Temperature Ionic Liquids. 2. Variation of Alkyl Chain Length in Imidazolium Cation. *J. Phys. Chem. B* **2005**, *109*, 6103−6110.
(54) Köddermann, T.; Paschek, D.; Ludwig, R. Ionic Liquids: Dissecting the Enthalpies of Vaporization. *ChemPhysChem* **2008**, *9*, 549−555.
(55) Morrow, T. I.; Maginn, E. J. Molecular Dynamics Study of the Ionic Liquid 1-n-Butyl-3-methylimidazolium Hexafluorophosphate. *J. Phys. Chem. B* **2002**, *106*, 12807−12813.
(56) Chaban, V. Polarizability Versus Mobility: Atomistic Force Field for Ionic Liquids. *Phys. Chem. Chem. Phys.* **2011**, *13*, 16055−16062.
(57) Men, S.; Lovelock, K. R. J.; Licence, P. X-ray Photoelectron Spectroscopy of Pyrrolidinium-based Ionic Liquids: Cation-anion Interactions and a Comparison to Imidazolium-based Analogues. *Phys. Chem. Chem. Phys.* **2011**, *13*, 15244−15255.

(58) Hurisso, B. B.; Lovelock, K. R. J.; Licence, P. Amino Acid-based Ionic Liquids: Using XPS to Probe the Electronic Environment Via Binding Energies. *Phys. Chem. Chem. Phys.* **2011**, *13*, 17737−17748.
(59) Liu, Z.; Wu, X.; Wang, W. A Novel United-atom Force Field for Imidazolium-based Ionic Liquids. *Phys. Chem. Chem. Phys.* **2006**, *8*, 1096−1104.
(60) Zhong, X.; Liu, Z.; Cao, D. Improved Classical United-Atom Force Field for Imidazolium-Based Ionic Liquids: Tetrafluoroborate, Hexafluorophosphate, Methylsulfate, Trifluoromethylsulfonate, Acetate, Trifluoroacetate, and Bis(trifluoromethylsulfonyl)amide. *J. Phys. Chem. B* **2011**, *115*, 10027−10040.
(61) Tsuzuki, S.; Matsumoto, H.; Shinoda, W.; Mikami, M. Effects of Conformational Flexibility of Alkyl Chains of Cations on Diffusion of Ions in Ionic Liquids. *Phys. Chem. Chem. Phys.* **2011**, *13*, 5987−5993.
(62) Bagno, A.; D'Amico, F.; Saielli, G. Computer Simulation of Diffusion Coefficients of the Room-temperature Ionic Liquid [bmim][BF_4]: Problems with Classical Simulation Techniques. *J. Mol. Liq.* **2007**, *131*−*132*, 17−23.
(63) Bedrov, D.; Borodin, O.; Li, Z.; Smith, G. D. Influence of Polarization on Structural, Thermodynamic, and Dynamic Properties of Ionic Liquids Obtained from Molecular Dynamics Simulations. *J. Phys. Chem. B* **2010**, *114*, 4984−4997.
(64) Vatamanu, J.; Borodin, O.; Bedrov, D.; Smith, G. D. Molecular Dynamics Simulation Study of the Interfacial Structure and Differential Capacitance of Alkylimidazolium Bis(trifluoromethanesulfonyl)-imide [$C_n$mim][TFSI] Ionic Liquids at Graphite Electrodes. *J. Phys. Chem. C* **2012**, *116*, 7940−7951.
(65) Vatamanu, J.; Borodin, O.; Smith, G. D. Molecular Simulations of the Electric Double Layer Structure, Differential Capacitance, and Charging Kinetics for N-Methyl-N-propylpyrrolidinium Bis-(fluorosulfonyl)imide at Graphite Electrodes. *J. Phys. Chem. B* **2011**, *115*, 3073−3084.
(66) Vatamanu, J.; Borodin, O.; Smith, G. D. Molecular Insights into the Potential and Temperature Dependences of the Differential Capacitance of a Room-Temperature Ionic Liquid at Graphite Electrodes. *J. Am. Chem. Soc.* **2010**, *132*, 14825−14833.
(67) Koßmann, S.; Thar, J.; Kirchner, B.; Hunt, P. A.; Welton, T. Cooperativity in Ionic Liquids. *J. Chem. Phys.* **2006**, *124*, 174506.
(68) Schmidt, J.; Krekeler, C.; Dommert, F.; Zhao, Y.; Berger, R.; Delle Site, L.; Holm, C. Ionic Charge Reduction and Atomic Partial Charges from First-Principles Calculations of 1,3-Dimethylimidazolium Chloride. *J. Phys. Chem. B* **2010**, *114*, 6150−6155.
(69) Wendler, K.; Zahn, S.; Dommert, F.; Berger, R.; Holm, C.; Kirchner, B.; Delle Site, L. Locality and Fluctuations: Trends in Imidazolium-Based Ionic Liquids and Beyond. *J. Chem. Theory Comput.* **2011**, *7*, 3040−3044.
(70) Wendler, K.; Dommert, F.; Zhao, Y. Y.; Berger, R.; Holm, C.; Delle Site, L. Ionic Liquids Studied Across Different Scales: A Computational Perspective. *Faraday Discuss.* **2012**, *154*, 111−132.
(71) Blöchl, P. E. Electrostatic Decoupling of Periodic Images of Plane-wave-expanded Densities and Derived Atomic Point Charges. *J. Chem. Phys.* **1995**, *103*, 7422−7428.
(72) Dommert, F.; Holm, C. Refining Classical Force Fields for Ionic Liquids: Theory and Application to [MMIM][Cl]. *Phys. Chem. Chem. Phys.* **2013**, *15*, 2037−2049.
(73) Dommert, F.; Wendler, K.; Qiao, B.; Delle Site, L.; Holm, C. Generic Force Fields for Ionic Liquids. *J. Mol. Liq.* **2013**, http://dx.doi.org/10.1016/j.molliq.2013.09.001.
(74) Zhang, Y.; Maginn, E. J. A Simple AIMD Approach to Derive Atomic Charges for Condensed Phase Simulation of Ionic Liquids. *J. Phys. Chem. B* **2012**, *116*, 10036−10048.
(75) Manz, T. A.; Sholl, D. S. Improved Atoms-in-Molecule Charge Partitioning Functional for Simultaneously Reproducing the Electrostatic Potential and Chemical States in Periodic and Nonperiodic Materials. *J. Chem. Theory Comput.* **2012**, *8*, 2844−2867.
(76) Manz, T. A.; Sholl, D. S. Chemically Meaningful Atomic Charges That Reproduce the Electrostatic Potential in Periodic and Nonperiodic Materials. *J. Chem. Theory Comput.* **2010**, *6*, 2455−2468.
(77) Jasuja, H.; Zang, J.; Sholl, D. S.; Walton, K. S. Rational Tuning of Water Vapor and CO_2 Adsorption in Highly Stable Zr-Based MOFs. *J. Phys. Chem. C* **2012**, *116*, 23526−23532.
(78) Fang, H.; Kamakoti, P.; Ravikovitch, P. I.; Aronson, M.; Paur, C.; Sholl, D. S. First Principles Derived, Transferable Force Fields for CO_2 Adsorption in Na-exchanged Cationic Zeolites. *Phys. Chem. Chem. Phys.* **2013**, *15*, 12882−12894.
(79) Allen, F. H. The Cambridge Structural Database: A Quarter of a Million Crystal Structures and Rising. *Acta Crystallogr., Sect. B: Struct. Sci* **2002**, *58*, 380−388.
(80) Bruno, I. J.; Cole, J. C.; Edgington, P. R.; Kessler, M.; Macrae, C. F.; McCabe, P.; Pearson, J.; Taylor, R. New software for Searching the Cambridge Structural Database and Visualizing Crystal Structures. *Acta Crystallogr., Sect. B: Struct. Sci* **2002**, *58*, 389−397.
(81) Bruno, I.; Cole, J.; Lommerse, J.; Rowland, R.; Taylor, R.; Verdonk, M. IsoStar: A Library of Information About Nonbonded Interactions. *J. Comput. Aided Mol. Des.* **1997**, *11*, 525−537.
(82) Hutter, J.; Iannuzzi, M.; Schiffmann, F.; VandeVondele, J. CP2K: Atomistic Simulations of Condensed Matter Systems. *Wiley Interdiscip. Rev. Comput. Mol. Sci.* **2014**, *4*, 15−25.
(83) Goedecker, S.; Teter, M.; Hutter, J. Separable Dual-space Gaussian Pseudopotentials. *Phys. Rev. B* **1996**, *54*, 1703−1710.
(84) Campañá, C.; Mussard, B.; Woo, T. K. Electrostatic Potential Derived Atomic Charges for Periodic Systems Using a Modified Error Functional. *J. Chem. Theory Comput.* **2009**, *5*, 2866−2878.
(85) Bayly, C. I.; Cieplak, P.; Cornell, W.; Kollman, P. A. A Well-behaved Electrostatic Potential Based Method Using Charge Restraints for Deriving Atomic Charges: the RESP Model. *J. Phys. Chem.* **1993**, *97*, 10269−10280.
(86) Plimpton, S. Fast Parallel Algorithms for Short-Range Molecular Dynamics. *J. Comput. Phys.* **1995**, *117*, 1−19.
(87) Martin, M. G.; Siepmann, J. I. Transferable Potentials for Phase Equilibria. 1. United-Atom Description of n-Alkanes. *J. Phys. Chem. B* **1998**, *102*, 2569−2577.
(88) Zahn, S.; Bruns, G.; Thar, J.; Kirchner, B. What Keeps Ionic Liquids in Flow? *Phys. Chem. Chem. Phys.* **2008**, *10*, 6921−6924.
(89) Frisch, M. J.; Trucks, G. W.; Schlegel, H. B.; Scuseria, G. E.; Robb, M. A.; Cheeseman, J. R.; Scalmani, G.; Barone, V.; Mennucci, B.; Petersson, G. A. *Gaussian 09*, Revision D.01; Gaussian Inc.: Wallingford, CT, 2009.
(90) Dennington, R.; Keith, T.; Millam, J. *GaussView* Version 5; Semichem Inc.: Shawnee Mission, KS, 2009.
(91) Hoover, W. G. Canonical Dynamics: Equilibrium Phase-space Distributions. *Phys. Rev. A* **1985**, *31*, 1695−1697.
(92) Martínez, L.; Andrade, R.; Birgin, E. G.; Martínez, J. M. PACKMOL: A Package for Building Initial Configurations for Molecular Dynamics Simulations. *J. Comput. Chem.* **2009**, *30*, 2157−2164.
(93) Macrae, C. F.; Edgington, P. R.; McCabe, P.; Pidcock, E.; Shields, G. P.; Taylor, R.; Towler, M.; van de Streek, J. Mercury: Visualization and Analysis of Crystal Structures. *J. Appl. Crystallogr.* **2006**, *39*, 453−457.
(94) Humphrey, W.; Dalke, A.; Schulten, K. VMD: Visual Molecular Dynamics. *J. Mol. Graphics* **1996**, *14*, 33−38.
(95) Dibrov, S. M.; Kochi, J. K. Crystallographic View of Fluidic Structures for Room-temperature Ionic Liquids: 1-butyl-3-methylimidazolium hexafluorophosphate. *Acta Crystallogr., Sect. C* **2006**, *62*, o19−o21.
(96) Holbrey, J. D.; Reichert, W. M.; Nieuwenhuyzen, M.; Johnson, S.; Seddon, K. R.; Rogers, R. D. Crystal Polymorphism in 1-butyl-3-methylimidazolium halides: Supporting Ionic Liquid Formation by Inhibition of Crystallization. *Chem. Commun.* **2003**, 1636−1637.
(97) Tokuda, H.; Tsuzuki, S.; Susan, M. A. B. H.; Hayamizu, K.; Watanabe, M. How Ionic Are Room-Temperature Ionic Liquids? An Indicator of the Physicochemical Properties. *J. Phys. Chem. B* **2006**, *110*, 19593−19600.
(98) Li, J.-G.; Hu, Y.-F.; Ling, S.; Zhang, J.-Z. Physicochemical Properties of [C_6mim][PF_6] and [C_6mim][$(C_2F_5)_3PF_3$] Ionic Liquids. *J. Chem. Eng. Data* **2011**, *56*, 3068−3072.

(99) Seddon, K. R.; Annegret, S.; María-José, T. *Clean Solvents*; American Chemical Society: Washington, DC, 2002; Chapter 5, pp 34−49.
(100) He, R.-H.; Long, B.-W.; Lu, Y.-Z.; Meng, H.; Li, C.-X. Solubility of Hydrogen Chloride in Three 1-Alkyl-3-methylimidazolium Chloride Ionic Liquids in the Pressure Range (0 to 100) kPa and Temperature Range (298.15 to 363.15) K. *J. Chem. Eng. Data* **2012**, *57*, 2936−2941.
(101) Swiderski, K.; McLean, A.; Gordon, C. M.; Vaughan, D. H. Estimates of Internal Energies of Vaporisation of Some Room Temperature Ionic Liquids. *Chem. Commun.* **2004**, 2178−2179.
(102) Lee, S. H.; Lee, S. B. The Hildebrand Solubility Parameters, Cohesive Energy Densities and Internal Energies of 1-alkyl-3-methylimidazolium-based Room Temperature Ionic Liquids. *Chem. Commun.* **2005**, 3469−3471.
(103) Xu, W.-G.; Li, L.; Ma, X.-X.; Wei, J.; Duan, W.-B.; Guan, W.; Yang, J.-Z. Density, Surface Tension, and Refractive Index of Ionic Liquids Homologue of 1-Alkyl-3-methylimidazolium Tetrafluoroborate $[C_n\text{mim}][BF_4]$ (n = 2,3,4,5,6). *J. Chem. Eng. Data* **2012**, *57*, 2177−2184.
(104) Borodin, O. Relation Between Heat of Vaporization, Ion Transport, Molar Volume, and Cation-Anion Binding Energy for Ionic Liquids. *J. Phys. Chem. B* **2009**, *113*, 12353−12357.
(105) Deyko, A.; Hessey, S. G.; Licence, P.; Chernikova, E. A.; Krasovskiy, V. G.; Kustov, L. M.; Jones, R. G. The Enthalpies of Vaporisation of Ionic Liquids: New Measurements and Predictions. *Phys. Chem. Chem. Phys.* **2012**, *14*, 3181−3193.
(106) Zaitsau, D. H.; Kabo, G. J.; Strechan, A. A.; Paulechka, Y. U.; Tschersich, A.; Verevkin, S. P.; Heintz, A. Experimental Vapor Pressures of 1-Alkyl-3-methylimidazolium Bis-(trifluoromethylsulfonyl)imides and a Correlation Scheme for Estimation of Vaporization Enthalpies of Ionic Liquids. *J. Phys. Chem. A* **2006**, *110*, 7303−7306.
(107) Emel'yanenko, V. N.; Verevkin, S. P.; Heintz, A.; Schick, C. Ionic Liquids. Combination of Combustion Calorimetry with High-Level Quantum Chemical Calculations for Deriving Vaporization Enthalpies. *J. Phys. Chem. B* **2008**, *112*, 8095−8098.
(108) Deyko, A.; Lovelock, K. R. J.; Corfield, J.-A.; Taylor, A. W.; Gooden, P. N.; Villar-Garcia, I. J.; Licence, P.; Jones, R. G.; Krasovskiy, V. G.; Chernikova, E. A.; Kustov, L. M. Measuring and Predicting $\Delta_{vap}H_{298}$ Values of Ionic Liquids. *Phys. Chem. Chem. Phys.* **2009**, *11*, 8544−8555.
(109) Bhargava, B. L.; Klein, M. L.; Balasubramanian, S. Structural Correlations and Charge Ordering in a Room-Temperature Ionic Liquid. *ChemPhysChem* **2008**, *9*, 67−70.
(110) Payal, R. S.; Balasubramanian, S. Homogenous Mixing of Ionic Liquids: Molecular Dynamics Simulations. *Phys. Chem. Chem. Phys.* **2013**, *15*, 21077−21083.
(111) Freire, M. G.; Carvalho, P. J.; Fernandes, A. M.; Marrucho, I. M.; Queimada, A. J.; Coutinho, J. A. Surface Tensions of Imidazolium Based Ionic Liquids: Anion, Cation, Temperature and Water Effect. *J. Colloid Interface Sci.* **2007**, *314*, 621−630.
(112) Tokuda, H.; Hayamizu, K.; Ishii, K.; Susan, M. A. B. H.; Watanabe, M. Physicochemical Properties and Structures of Room Temperature Ionic Liquids. 1. Variation of Anionic Species. *J. Phys. Chem. B* **2004**, *108*, 16593−16600.
(113) Kanakubo, M.; Harris, K. R.; Tsuchihashi, N.; Ibuki, K.; Ueno, M. Effect of Pressure on Transport Properties of the Ionic Liquid 1-Butyl-3-methylimidazolium Hexafluorophosphate. *J. Phys. Chem. B* **2007**, *111*, 2062−2069.
(114) Urahata, S. M.; Ribeiro, M. C. C. Single Particle Dynamics in Ionic Liquids of 1-alkyl-3-methylimidazolium Cations. *J. Chem. Phys.* **2005**, *122*, 024511.